

# Offset between dark matter and ordinary matter: evidence from a sample of 38 lensing clusters of galaxies

HuanYuan Shan<sup>1,6\*</sup>, Bo Qin<sup>1\*</sup>, Bernard Fort<sup>2</sup>, Charling Tao<sup>3</sup>, Xiang-Ping Wu<sup>1</sup>  
and HongSheng Zhao<sup>1,4,5</sup>

<sup>1</sup>National Astronomical Observatories, Chinese Academy of Sciences, Beijing 100012, China

<sup>2</sup>UPMC Université Paris 06, UMR7095, Institut d'Astrophysique de Paris, F-75014, Paris, France

<sup>3</sup>Centre de Physique des Particules de Marseille, CNRS/IN2P3-Luminy and Université de la Méditerranée, Case 907, F-13288 Marseille Cedex 9, France

<sup>4</sup>SUPA, University of St Andrews, KY16 9SS, UK

<sup>5</sup>Leiden University, Sterrewacht and Instituut-Lorentz, Niels-Bohrweg 2, 2333 CA, Leiden, The Netherlands

<sup>6</sup>Department of Astronomy, School of Physics, Peking University, Beijing, 100871, China

Accepted . . . . Received . . . . ; in original form . . . .

## ABSTRACT

We compile a sample of 38 galaxy clusters which have both X-ray and strong lensing observations, and study for each cluster the projected offset between the dominant component of baryonic matter center (measured by X-rays) and the gravitational center (measured by strong lensing). Among the total sample, 45% clusters have offsets  $> 10''$ . The  $> 10''$  separations are significant, considering the arcsecond precision in the measurement of the lensing/X-ray centers. This suggests that it might be a common phenomenon in unrelaxed galaxy clusters that gravitational field is separated spatially from the dominant component of baryonic matter. It also has consequences for lensing models of unrelaxed clusters since the gas mass distribution may differ from the dark matter distribution and give perturbations to the modeling. Such offsets can be used as a statistical tool for comparison with the results of  $\Lambda$ CDM simulations and to test the modified dynamics.

**Key words:** dark matter-gravitational lensing-X-rays: galaxies: clusters

## 1 INTRODUCTION

Seventy years after Zwicky's first piece of evidence for dark matter (DM) in galaxy clusters, the physics model for DM still remains ambiguous, ranging from Weakly-Interacting Massive Particles (WIMPs) to gravity-modifying Tensor-Vector-Scalar fields (TeVeS, Bekenstein 2004). In-between these seemingly conflicting theories, we also have models where the DM changes properties in different environments due to gravitational polarization or interactions with a dark energy field (Blanchet & Le Tiec 2009, Li & Zhao 2009). These in-between DM models explain why DM in galaxies seems to satisfy the MOND formulae of Milgrom (1983) with a common empirical scale  $a_0 \sim \sqrt{\Lambda} \sim 10^{-10} \text{m s}^{-2}$  found by fitting galaxy rotation curves. They are also consistent with the cosmic microwave background, and the late time dark energy effect  $\Lambda$  or order  $a_0^2$ .

MOND has gained enormous momentum, partly for its success in making reasonable stable galaxies and explaining galactic phenomenology (e.g., Wang et al. 2008; Wu et al. 2009; Gentile et al. 2009). MOND can also give high velocity encounters of galaxy clusters (Llinares et al. 2009). However, it does not

fully account for the discrepancy between the X-ray and dynamical mass in rich clusters of galaxies (Gerbal et al. 1992; The & White 1988; Aguirre, Schaye & Quataert 2001; Sanders 2003; Tian, Hoekstra, & Zhao 2009), which Sanders (2003) explained by introducing a 2 eV neutrino component. We also should note that the environmental-dependent DM of Li & Zhao (2009) and the DM dipoles of Blanchet & Le Tiec (2009), both mimic MOND for galaxies, might resolve the apparent contradiction of MOND for clusters.

A big challenge to modified gravity is the observations of the bullet cluster 1E0657-56 (Bradac et al. 2006; Clowe et al. 2006; Markevitch et al. 2006). Weak lensing observations of the bullet cluster, combined with earlier X-ray measurements, clearly indicated that the gravitational field of the cluster has an obvious offset from its ordinary matter distribution.

One immediate question one may ask is: Is the bullet cluster the only system that uniquely shows the spatial separation between dark and ordinary matter? Is the phenomenon of DM-baryon separation so rare in the universe, or could it be more common?

In galaxy clusters, most baryons (or ordinary matter) exist in the form of diffuse X-ray emitting gas. The stellar component is larger at the cluster center where bright galaxies are concentrated but DM is still the dominant component. This has been demonstrated by Gavazzi et al. (2003) and Gavazzi (2005): for the in-

\* E-mail: shanhuany@gmail.com, qinbo@bao.ac.cn

ner  $\lesssim 100$  kpc regions of a lensing cluster, the stellar component only occupies a few percent of the total mass. Therefore, the X-ray images could be used as a reasonable approximation of the ordinary matter distribution in a cluster. X-ray observations measure directly the ordinary matter distributions, while the total projected mass distributions (mainly DM) can be measured by gravitational lensing. Thus, a comparison between X-ray and lensing observations of galaxy clusters potentials may unveil possible differences between dark and ordinary matter distributions, just as the observations of the bullet cluster have revealed.

Strong lensing has the potential to determine the cluster mass center with arcsecond precision. The  $0.5''$  high spatial resolution of the Chandra X-ray satellite means that we may determine an accurate position of a cluster’s baryonic center, though the X-ray data processing may eventually give rise to a larger uncertainty of no more than a few arcseconds (see e.g. Smith et al. 2005). Thus, we can compare the gravitational and baryonic centers of galaxy clusters by investigating a fairly large sample. If the gravitational center of a lensing cluster does not match the ordinary matter center, we could say that a separate DM component might exist. Indeed we expect this result for cluster on-going major merger.

Offsets between lensing and X-ray centers were incidently noticed a decade ago by Allen (1998) when he was studying a sample of 13 clusters. However, no attempt has been made to use such offsets as a dynamical signature, which might be used as quantitative measure of the quality of the DM model by comparing with similar statistics coming from  $\Lambda$ CDM simulations.

In this paper, we compile a sample of 38 galaxy clusters that have both strong lensing (SL) and X-ray observations. We carefully check the lensing hypothesis and location of the main potential of the lens if several deflectors are considered. Combining the lensing data with X-ray data, we obtain for each cluster an offset between the lensing center and X-ray center on the projected plane. We use this offset as an “indicator” to describe the dark matter-ordinary matter separation. Our data strongly support the idea that the gravitational potential in clusters is mainly due to a non-baryonic fluid, and any exotic field in gravitational theory must resemble that of CDM fields very closely. Moreover, we find that unrelaxed clusters have larger offsets than relaxed clusters.

Interestingly, simulations of CDM+baryon for galaxy clusters in the standard  $\Lambda$ CDM cosmology has recently found offsets between the baryonic and DM centers in clusters (Forero-Romero et al. 2010). The offset can be as large as 100 kpc. This roughly supports our findings, though the details of the cluster distribution functions between the simulations and our observational data show some difference.

## 2 CLUSTER SAMPLE AND RESULTS

The sample of 38 clusters is listed in Table 1, which shows the positions of the lensing/optical and X-ray centroids on the projected plane, the two-dimensional offsets between the lensing and X-ray centers (given in arcsecond), and the corresponding angular diameter distances (in kpc) calculated in the  $\Lambda$ CDM cosmology. The lensing/optical data are from the HST WFPC2 archive, the SDSS survey and some other independent observations. Most of the X-ray data are from the Chandra archive, except for 13 clusters from ROSAT (marked with “9”, “11”, “15” in the Ref.B column). For clusters with several DM clumps, we choose the one with the largest X-ray temperature and give the corresponding X-ray center in the sample. The clusters in our table are classified from their

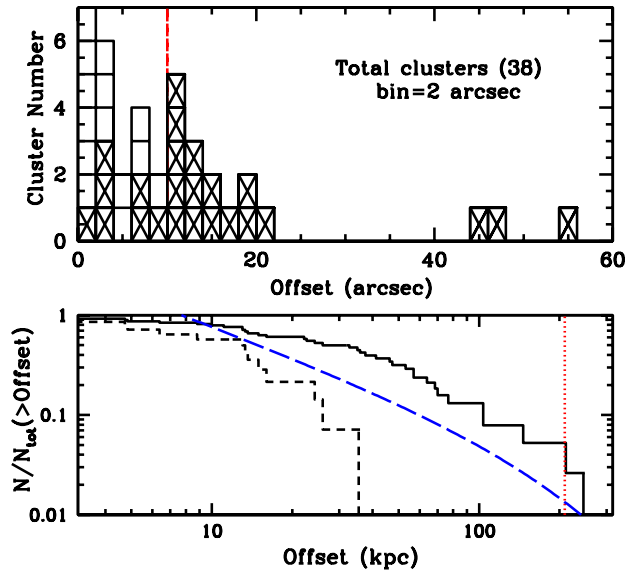


**Figure 1.** *Upper panel:* Histogram of the cluster distribution as a function of the offset between the lensing center and X-ray center, for a sample of 38 galaxy clusters with both strong lensing and X-ray observations. The crossed boxes represent unrelaxed clusters. The red vertical dashed line marks the offset of  $10''$ . *Lower panel:* Cumulative distribution of the total clusters (solid line) and relaxed clusters (dashed line) as a function of the 2-D physical separation between lensing and X-ray centers. The red vertical dotted line corresponds to the bullet cluster offset. The blue long dashed line  $P_{2D} = 0.04 \left(\frac{d}{200}\right)^{-1} \exp\left(\frac{d}{200}\right)$  shows the Forero-Romero et al. (2010) simulation results.

X-ray morphologies as relaxed clusters (with cooling flows) and unrelaxed clusters (which are dynamically unmaturing). This definition has been used in the literature by Allen (1999), Wu (2000), Baldi et al (2007), and Dunn & Fabian (2008). Figure 1 shows the cluster number counts as a function of the offset (2-D separation between the lensing and X-ray centers).

The lensing centers of these clusters are always determined by their arcs and images’ positions. Remarkably about half of the best models for relaxed clusters have adopted the “Brightest Cluster Galaxy” (BCG) center of mass as the DM halo center. The BCG has a faint extended star halo with a distribution similar to that of the DM (same center and almost the same ellipticity and main axis orientation). For the case where the DM center is actually kept as a free parameter, the offset between the BCG and lensing center seems to be below  $1.5''$ . It is reasonable to consider the BCG center as the lensing center of relaxed clusters. As for the unrelaxed clusters which show larger offsets, the BCGs cannot be taken as a unique lensing center. Smith et al. (2005) show that the offset errors of the main potential of 7 unrelaxed clusters are with the typical value around  $2''$ , which includes uncertainties on the central coordinates of the cluster mass distribution in the relevant lens model with all the arcs and images’ positions.

The X-ray centers of the clusters are always determined by the weighted averaging of the pixel centers covering the cluster, which depends on the number of X rays in a pixel, the number of pixels and flux distribution used for the centroid determination. Lazzati & Chincarni (1998) have estimated the effect of pixel sizes on the centroid determined to be around a quarter of a pixel. For pixel

sizes equivalent to  $6''$ , the effect is less than  $2''$ . The error from the algorithm fit on the centroid can however be larger, but the authors claim that a value of  $5''$  is pretty conservative.

The X-ray center determination may be also dependent on the size of the region considered for the estimates, especially for unrelaxed clusters whose X-ray morphologies are not so regular compared with relaxed clusters. To test this, Maughan et al. (2008) have measured the “centroid shifts” for 115 X-ray clusters, following earlier work by Mohr et al. (1993), O’Hara et al. (2006) and Poole et al. (2006). The centroid shifts were determined in a series of circular apertures centered on the cluster X-ray peak, with the radius of the apertures decreasing in steps of 5% from  $R_{500}$  to  $0.05R_{500}$ . Maughan et al. (2008) found that the value of the centroid shift,  $w$ , ranges from a few tenths to a few of  $10^{-2}R_{500}$  in the sample. Typically  $R_{500} \sim 1$  Mpc for clusters. So this centroid shift is roughly equivalent to measuring the difference between the very extreme cases of the  $r \sim 0$  region and the  $r = 1$  Mpc region. For the clusters in our sample,  $w$  is typically a few arcsecs. For example, the unrelaxed clusters A68 and A209 have  $w = 4''$  and  $2''$  respectively. For the well-known unrelaxed bullet cluster,  $w = 8''$ .

Considering the above errors as a whole, we define our *Selection Criterion*—We only regard offsets larger than  $10''$  as being significant. This is a fairly conservative criterion if we consider lensing rays tracing with simulations like the Millennium (Hilbert et al. 2007). For systems with offsets much smaller than  $10''$ , observational uncertainties may start to play an important role as well as the lensing modeling errors, if external shear perturbations have not been well identified in the field.

One prominent feature of Figure 1 is that all the clusters with offsets  $> 10''$  are unrelaxed clusters, suggesting that the mechanism for this lensing/X-ray offset is probably related to dynamical relaxations, which is the same as the research about the offset between BCG/X-ray center (Sanderson et al. 2009). In total, there is a rather high percentage of clusters with obvious offsets — almost half of the clusters (45%) in the whole sample have offsets  $> 10''$ , and 3 clusters (or 8%) even have extraordinarily large separations of  $> 40''$ , indicating that such offsets may not be rare in unrelaxed clusters. Taking into account the fact that the observed offsets are only two-dimensional, the true separations (3-D) should be even higher (see the discussion section). In addition to the well-studied bullet cluster, which has an offset value of  $47.4''$ , clusters A2163, and A2744 also have very large offsets of  $44.0''$  and  $54.3''$ , respectively.

Our selection criterion of  $> 10''$  is mainly based on the errors in the lensing and X-ray measurements, which are typically about a few arcsecs. If we increase this threshold from  $10''$  to  $20''$ , then our sub-sample of large offset clusters will decrease drastically from 45% to only 10%. This is naturally expected, because the distribution (total number) of clusters decreases very rapidly with increasing offset. This trend is clearly demonstrated by the blue dashed curve in Figure 1 which is a result of numerical simulations. Also, dynamical relaxations will tend to reduce the offset in clusters, leading to more relaxed clusters. Interestingly, all of the four offset  $> 20''$  clusters are discovered at relatively high redshifts of  $z > 0.2$ .

We also note some peculiar cases in our sample. A370 seems made of two relaxed clusters along the same line of sight which have not yet merged. In such a case, despite the blending effect, we see two X-ray peaks at each BCG center (equivalent to lensing centers, c.f. the map of Kneib et al. 1993). In A370, the distance between the two equivalent potential wells is  $40''$  (according to the lens modeling). Bonamente et al. (2006) showed a map of

the blend emissions of two cluster lenses. A detailed study of the offset might involve subdividing the sample according to different degrees of merging. Further studies of the ordinary matter offsets might involve subdividing the cluster sample according to different degrees of merging by considering the velocity distributions of galaxy members. A1682 contains two BCG, and only one of them produces strong lensing arc. The small radius of the known arc (Sand et al. 2005) indicates that this is galaxy-scale lensing, and is not caused primarily by the dark matter core of the cluster. So it would be incorrect to use the SL center as the mass center of this cluster. The unrelaxed cluster A1914 only has one arc without redshift and counter-arc (Sand et al. 2005), which would result in large errors in SL center determination. The offset between SL and X-ray center is  $53.6''$ . Dahle et al. (2002) studied this cluster with weak lensing, and showed that the cluster has a triangle of bright elliptical (with probably two cD) galaxies. The weak lensing measurement places the center of mass of the cluster very close to the X-ray centroid, indicating that the SL is caused by one of the cD in a complex merging process involving several substructures and possible projection effects. For such a cluster the weak lensing appears representative of the cluster center on large scales. But without other multiple gravitational arcs around cDs it is not possible to conclude about the DM peaks at the cluster center. Only the BCG-X ray offset gives the signature of a merging process.

### 3 DISCUSSION AND CONCLUSIONS

The mass in stars of a cluster is small compared to its X-ray gas. Therefore the X-ray images can be used as a reasonable approximation of ordinary matter distribution in a cluster. Similarly the stellar mass component is not dominant in SL modeling even if it often seems the SL and stellar mass centers peak at the same place, the BCG center. Consequently we have used the X-ray images (which is the result of the diffuse intracluster X-ray gas) to find the center of ordinary matter distribution and the lensing mass to find the center of dark matter distribution. Indeed this is an approximation and we have explained that the error in the separation angle shall be much less than  $10''$ . Therefore the separation between DM and ordinary matter is highly significant for the unrelaxed clusters.

It is noticeable that all the clusters in our sample are clusters with  $z > 0.1$  (most of them have  $z > 0.2$ ). This selection effect is caused by strong lensing clusters because higher redshift clusters have higher lensing probabilities. In order to have high precision determinations of the gravitational center of clusters, we have to focus on strong lensing clusters—which means that our cluster sample has to be a high redshift sample instead of containing many local clusters. In principle, we should have a more unbiased sample with sufficient low redshift clusters which are measured by, e.g., high quality weak lensing.

However, current weak lensing determination of the lensing center is much less robust compared with strong lensing. Indeed, we have investigated clusters with both X-ray and weak lensing observations (but not strong lensing) and found the lensing/X-ray offsets. For example, cluster MS1054 (Jee et al. 2005) has an offset of  $19.5''$ . MS1008 (Ettori & Lombardi 2003) has an offset of  $5.43''$ . But unfortunately, the errors from weak lensing are much larger. Nevertheless, high quality weak lensing observations of clusters, especially low redshift clusters, will be of particular interest.

It should be noted that the offset here is only 2-D, i.e., the separation on the projected plane. The true separation (3-D) could be much larger. One extreme example is cluster CL0024+17. The

redshift distribution of the cluster's member galaxies revealed that the configuration of this cluster is along the line of sight (Czoske et al. 2001). Moreover, recent studies suggested that this cluster may have undergone a head-on collision along the line of sight (Jee et al. 2007; Qin et al. 2008). So its 3-D separation is probably much larger than the 2-D offset in Table 1. The other extreme case is the bullet cluster, where the configuration (as well as the head-on collision) is roughly on the projected plane, indicating that its 3-D separation is close to the 2-D offset.

The bullet cluster has provided us a system that clearly shows the existence of a DM component. RX J1347.5-1145 (Bradac et al. 2008) is similar but with another line of sight projection: the east massive clump has lost all its X-ray gas. For the bullet cluster, Angus et al. (2007) have pointed out that MOND could be rescued if DM is made of 2 eV neutrinos, following the  $\mu$ HDM model introduced by Sanders (2003). Indeed such an observation seems to match structure formation in both  $\mu$ HDM and  $\Lambda$ CDM cosmologies. Meanwhile, Knebe et al. (2009) found that MOND can in principle produce offsets of effective DM, but the offsets are often small, about 1 kpc.

There are also implications in the CDM framework. The significant offset found here is a signal of the merging process and is a measure of the departure from equilibrium, and consequently the X-ray determined dynamical mass based on equilibrium would under-predict compared to lensing-determined mass, which does not use assumptions of equilibrium (Allen 1998; Smith et al. 2005; Zu Hone et al. 2009).

Concerning the SL modeling, it is necessary to identify all the mass distribution that might induce an external shear on the arc system. But it might be also important to include the shear-like perturbation of an offset gas component, a possible systematic effect neglected in previous models. All SL modeling (except the bullet cluster) has been continuously done with a smooth halo component which includes DM component plus the gas with the implicit hypothesis that the gas follows the DM distribution, which is not true except for a fully relaxed cluster. Most sophisticated models also considered the mass perturbation of the stellar component and sub-halo associated to early type galaxy members (sometimes with a separate stellar component of the BCG) to improve the modeling of the arc configuration (Kneib et al. 1996; Meneghetti et al. 2003; Keeton 2003; Limousin et al. 2007; Natarajan et al. 2007). Despite that Allen (1998) has explicitly noted the offset of the ordinary gas matter, it is remarkable that nobody has considered the SL modeling with an offset of a large proportion of the ordinary mass, on the same footing as the member galaxies effect. In this paper, we strongly argue that the offset of the ordinary gas matter, which represents 10% – 20% of the total cluster mass, should be figured out explicitly for unrelaxed clusters.

In summary, our finding of a high percentage (45%) of clusters with offsets  $> 10''$  in the whole sample suggests that it might be a common phenomenon that in unrelaxed galaxy clusters the gravitational field is more or less separated from the ordinary matter distribution. Such separation is best explained if a non-baryonic matter component (DM) does exist. The separations are probably due to dynamical relaxations, as all the clusters with offsets  $> 10''$  in the sample are unrelaxed clusters.

Indeed simulations of the cluster gas in the CDM framework do show the existence of the large offsets (Ferreiro-Romero et al. 2010). The simulation (Gottloeber & Yepes 2007), called The Marenstrum Universe, was run using the code GADGET2 and followed the adiabatic evolution of gas and dark matter from  $z = 40$  to  $z = 0$  in a comoving cube of  $500h^{-1}$  Mpc. The simulation predicts a

median offset of about 18 kpc, which is in general agreement with our whole sample. Nevertheless, the profiles of these offset distributions (i.e., cluster distribution functions with respect to offset) are non-identical, as shown in Figure 1. A K-S test shows that the significance of differences are 99.2% and 99.6% for the whole sample and the subsample of relaxed clusters, respectively.

From Figure 1, the biggest difference between the simulation results and our total cluster sample is that our sample has more clusters with large offsets. The main reasons could be as follows:

(1) Our sample of lensing clusters is biased towards higher redshift while the simulations are not. Obviously, dynamical relaxation will reduce the offset in clusters, leading to fewer clusters with large offsets as compared with the high redshift sample. In other words, most clusters in our sample have  $z > 0.2$ , and it is possible that these high redshift clusters are not fully evolved dynamically as compared with low redshift clusters. Also our sample of 38 clusters is still not big enough, and a larger sample is needed to draw a more robust conclusion.

(2) When a cluster of a given total mass is not fully relaxed and has still large merging clumps about to merge at the center, the length of the caustic lines is increased as compared to a fully relaxed cluster. So it could result in a higher probability to produce lensing arcs, as has been pointed out by Meneghetti et al. (2007). Therefore the fact that we observe more distant clusters which are less relaxed than at  $z = 0$  has a double bias effect.

(3) The gas physics in galaxy clusters is complicated and less well-understood. Obviously, different treatment of the gas could result in different cluster mass profiles and baryonic distributions, which could give different offset values.

There are other possible explanations, e.g., the merging history model may need to be revised, or the simulations may not have the complete recipes for the physics of DM. Another example is that DM could be possibly coupled to a dark energy scalar field, which distorts the non-linear dynamics at the centers of halos without ruining the large scale success of the standard cold DM. In short, more comparisons of new simulations and larger samples of clusters would be very rewarding in the future, as the offsets observed here provide astrophysicists a new quantitative tool to evaluate different cosmologies.

## Acknowledgments

We thank Raphael Gavazzi, Zhi-Ying Huo, Marceau Limousin and Shude Mao for discussions, and an anonymous referee for helpful suggestions. HYS and BQ are grateful to the CPPM for hospitality. HSZ acknowledges partial support from the Dutch NWO visitor's grant #040.11.089 to Henk Hoekstra. This work was supported by the National Basic Research Program of China (973 Program) under grant No. 2009CB24901, and CAS grants KJCX3-SYW-N2 and KJCX2-YW-N32.

## REFERENCES

- Aguirre, A., Schaye, J., & Quataert, E., 2001, *ApJ*, 561, 520
- Allen, S.W., 1998, *MNRAS*, 296, 392
- Angus, G., Shan, H. Famaey, B., & Zhao, H.S., 2007, *ApJ*, 654, 13
- Baldi, A., et al., 2007, *ApJ*, 666, 835
- Bekenstein, 2004, *Phys. Rev. D*, 70, 3509
- Bonamente, M., et al., 2006, *ApJ*, 647, 25
- Blanchet, L., & Le Tiec, A., 2009, *Phy. Rev. D*, 80, 023524

- Bradac, M. B., Clowe, D., Gonzalez, A. H., et al., 2006, *ApJ*, 652, 937
- Bradac, M., Schrabback, T., Erben, T. et al., 2008, *ApJ*, 681, 187
- Campusano, L. E., et al., 2001, *A&A*, 378, 394
- Clowe, D., et al., 2006, *ApJ*, 648, 109
- Czoske, O., et al., 2001, *A&A*, 372, 391
- Dahle, H.; Kaiser, N., Irgens, R. J., Lilje, P. B., & Maddox, S. J., 2002, *ApJS*, 139, 313
- Dunn, R. J. H., & Fabian, A. C., 2008, *MNRAS*, 385, 757
- Ettori, S., & Lombardi, M., 2003, *A&A*, 398, 5
- Forero-Romero, J.E., Gottlober, S., & Yepes, G., 2010, *ApJL*, submitted
- Gavazzi, R., Fort, B., Mellier, Y., Pello, R., & Dantel-Fort, M., 2003, *A&A*, 403, 11
- Gavazzi, R., 2005, *A&A*, 443, 793
- Gerbal, D., Durret, F., Lachieze-Rey, M., & Lima-Neto, G., 1992, *A&A*, 262, 395
- Gioia, I. M., et al., 1998, *ApJ*, 497, 573
- Gentile, G., Famaey, B., Zhao, H.S., & Salucci, P., 2009, *Nature*, 1 Oct 2009
- Gottloeber, S., & Yepes, G., 2007, *ApJ*, 664, 117
- Hilbert, S., White, S., Hartlap, J., & Schneider, P., 2007, *MNRAS*, 382, 121
- Jee, M.J., et al., 2005, *ApJ*, 634, 813
- Jee, M.J., et al., 2007, *ApJ*, 661, 728
- Kausch, W., et al., 2004, Proc. of "Baryons in Dark Matter Halos", ed. Dettmar, R., et al., SISSA, Proc. of Science, <http://pos.sissa.it>
- Kempner, J.C., & David, L.P., 2004, *MNRAS*, 349, 385
- Keeton, C., 2003, *ApJ*, 584, 664
- Knebe, A., Llinares, C., Zhao, H.S., & Wu, X., 2009, *ApJ*, 703, 2285
- Kneib, J.-P., Mellier, Y., Fort, B., & Mathez, G., 1993, *A&A*, 273, 367
- Kneib, J.-P., et al., 1996, *ApJ*, 471, 643
- Lazzati, D., & Chincarini, G., 1998, *A&A*, 339, 52
- Li, B., & Zhao, H.S., 2009, *Phys. Rev. D*, vol. 80, Issue 6, id. 064007
- Limousin, M., et al., 2007, *ApJ*, 668, 643
- Llinares, C., Zhao, H.S., & Knebe, A., 2009, *MNRAS*, 396, 109
- Markevitch, M. 2006, in *ESA Special Publication*, Vol. 604, *The X-ray Universe 2005*, ed. A. Wilson, 723
- Maughan, B.J., Jones, C., Forman, W., & Van Speybroeck, L., 2008, *ApJS*, 174, 117
- Meneghetti, M., Bartelmann, M., & Moscardini, L., 2003, *MNRAS*, 346, 67
- Meneghetti, M., et al., 2007, *A&A*, 461, 25
- Milgrom, M., 1983, *ApJ*, 270, 365
- Mohr, J. J., Fabricant, D. G., & Geller, M. J. 1993, *ApJ*, 413, 492
- Morrison, G.E., et al., 2003, *ApJS*, 146, 267
- Newbury, & Fahlman, 1999, arXiv: astro-ph/9905254
- Natarajan, P., De Lucia, G., & Springel, V., 2007, *MNRAS*, 376, 180
- O'Hara, T. B., Mohr, J. J., Bialek, J. J., & Evrard, A. E. 2006, *ApJ*, 639, 64
- Ota, N., & Mitsuda, K., 2004, *A&A*, 428, 757
- Paulin-Henriksson, S., et al., 2007, *A&A*, 467, 427
- Poole, G. B., Fardal, M. A., Babul, A., McCarthy, I. G., Quinn, T., & Wadsley, J., 2006, *MNRAS*, 373, 881
- Qin, B., Shan, H.-Y., & Tilquin, A., 2008, *ApJ*, 679, L81
- Radovich, M., Puddu, E., Romano, A., Grado, A., & Getman, F., 2008, arXiv: astro-ph/0804.4652
- Sand, D. J., Treu, T., Ellis, R. S., & Smith G. P., 2005, *ApJ*, 627, 32
- Sanders, R.H., 2003, *MNRAS*, 342, 901
- Sanderson, A., Edge, A., & Smith, G. P., 2009, *MNRAS*, 398, 1698
- Smith, G. P., et al., 2005, *MNRAS*, 359, 417
- The, L.S., & White, S.D.M., 1988, *AJ*, 95, 1642
- Tian, L., Hoekstra, H., & Zhao, H.S., 2009, *MNRAS*, 393, 885
- Wang, Y., Wu, X., & Zhao, H.S., 2008, *ApJ*, 677, 1033
- Wu, X.-P., 2000, *MNRAS*, 316, 299
- Wu, X., Zhao, H.S., Wang, Y., Llinares, C., & Knebe, A., 2009, *MNRAS*, 396, 109
- Zhao, H.S., 2007, *ApJ*, 671, L1
- Zu Hone, J.A., et al., 2009, *ApJ*, 699, 1004

**Table 1.** Offsets between the lensing centroids and X-ray centroids of a sample of 38 clusters. The lensing centroid data are taken from the HST WFPC2 archive, SDSS survey and some other independent measurements of lensing clusters. The X-ray centroid data are taken from the Chandra archive (except for 13 clusters denoted by “9”, “11”, “15” in Ref.B that are taken from the ROSAT archive). Ref.A and Ref.B give the references of the lensing and X-ray data respectively. The last column shows the classification of the clusters: “R/U” means relaxed/unrelaxed.

Cluster	$z_{\text{cluster}}$	Lensing/optical centroid		Ref.A	X-ray centroid		Ref.B	Offset		Class
		R.A.	Dec.		R.A.	Dec.		(arcsec)	(kpc)	
1E0657-56	0.296	06 58 35.3	-55 56 56.3	1	06 58 30.2	-55 56 35.9	1	47.4	209.2	U
A68	0.255	00 37 06.9	+09 09 23.3	3	00 37 06.2	+09 09 33.2	12	14.3	56.7	U
A209	0.206	01 31 52.5	-13 36 40.5	3,4	01 31 53.5	-13 36 46.1	13	15.6	52.7	U
A267	0.230	01 52 42.0	+01 00 26.2	3	01 52 42.1	+01 00 35.7	12	9.62	35.3	U
A370	0.375	02 39 53.1	-01 34 54.8	2,5	02 39 53.2	-01 34 35.0	12	19.9	102.7	U
A383	0.187	02 48 03.4	-03 31 45.2	3	02 48 03.4	-03 31 46.2	13	1.0	3.13	R
A586	0.170	07 32 20.3	+31 38 00.1	2	07 32 20.2	+31 37 55.6	12	4.68	13.6	R
A697	0.282	08 42 57.6	+36 21 59.1	2	08 42 57.8	+36 21 57.2	13	3.07	13.1	U
A773	0.217	09 17 53.4	+51 43 37.2	3	09 17 52.8	+51 43 40.4	13	6.43	22.6	U
A963	0.206	10 17 03.6	+39 02 49.2	3	10 17 03.7	+39 02 56.2	14	7.10	24.0	U
A1682	0.234	13 06 49.9	+46 33 33.5	2, 17, 18	13 06 51.1	+46 33 29.5	13	12.6	46.9	U
A1689	0.183	13 11 29.5	-01 20 27.6	6	13 11 29.5	-01 20 28.2	12	0.60	1.85	U
A1763	0.228	13 35 20.1	+41 00 04.0	3	13 35 20.0	+40 59 53.8	14	10.3	37.6	U
A1835	0.252	14 01 02.1	+02 52 42.3	3	14 01 02.0	+02 52 41.7	12	1.61	6.33	R
A1914	0.171	14 26 01.0	+37 49 45.0	2, 20	14 26 01.2	+37 49 34.0	13	11.3	32.9	U
A2204	0.151	16 32 46.9	+05 34 33.1	2	16 32 46.9	+05 34 31.9	12	1.20	3.15	R
A2163	0.203	16 15 49.1	-06 08 43.0	15, 19	16 15 46.2	-06 08 51.3	12	44.0	146.9	U
A2218	0.176	16 35 49.3	+66 12 45.3	3	16 35 51.9	+66 12 34.5	12	19.1	56.9	U
A2219	0.228	16 40 19.8	+46 42 41.7	3	16 40 20.2	+46 42 31.2	14	11.3	41.2	U
A2259	0.164	17 20 09.7	+27 40 07.4	2	17 20 08.5	+27 40 11.0	12	16.3	45.9	U
A2261	0.224	17 22 27.2	+32 07 57.5	2	17 22 27.1	+32 07 57.8	12	1.31	4.72	R
A2294	0.178	17 24 12.6	+85 53 11.6	2	17 24 09.6	+85 53 11.0	13	3.28	9.87	U
A2390	0.228	21 53 36.9	+17 41 43.4	2	21 53 36.5	+17 41 45.2	14	6.00	21.9	U
A2744	0.308	00 14 20.8	-30 24 03.0	15	00 14 18.7	-30 23 16.0	16	54.3	246.3	U
AC114	0.313	22 58 48.3	-34 48 07.2	2,7	22 58 49.2	-34 48 27.0	14	22.7	104.1	U
CL0024	0.395	00 26 35.0	+17 09 43.0	8	00 26 35.9	+17 09 40.0	14	13.2	70.4	U
MS0016	0.541	00 18 33.6	+16 26 16.0	2	00 18 33.6	+16 26 14.6	14	1.40	8.90	R
MS0440	0.190	04 43 09.7	+02 10 19.5	2	04 43 09.8	+02 10 19.5	9	1.50	4.89	R
MS0451	0.550	04 54 10.6	-03 00 50.7	2	04 54 11.4	-03 00 52.7	12	12.1	76.8	U
MS1137	0.782	11 40 22.3	+66 08 14.1	2	11 40 22.3	+66 08 16.1	12	2.00	14.9	R
MS1358	0.329	13 59 50.5	+62 31 06.8	2	35 59 50.6	+62 31 04.1	12	2.79	13.2	R
MS1455	0.258	14 57 15.1	+22 20 34.9	2,10	14 57 15.0	+22 20 37.3	14	2.77	11.1	U
MS1621	0.426	16 23 35.2	+26 34 28.2	2	16 23 35.7	+26 34 19.0	14	11.4	63.6	U
MS2053	0.580	20 56 21.4	-04 37 50.9	2	20 56 20.7	-04 37 51.6	14	10.5	69.1	U
MS2137	0.313	21 40 14.9	-23 39 39.5	2,10	21 40 15.2	-23 39 41.0	14	5.70	26.1	R
PKS0745	0.103	07 47 31.3	-19 17 40.0	2	07 47 31.4	-19 17 46.2	14	6.82	12.9	R
RXJ1347	0.451	13 47 30.7	-11 45 11.0	15	13 47 30.6	-11 45 08.6	12	2.81	16.2	R
RBS864	0.291	10 23 39.3	+04 11 17.0	11	10 23 39.6	+04 11 10.0	11	8.32	36.3	R

Notes:

<sup>a</sup> Units of R.A. are hours, minutes, and seconds, and units of Dec. are degrees, arcminutes, and arcseconds, respectively.

<sup>b</sup> References: (1) Clowe et al. 2006; Bradac et al. 2006; (2) Sand et al. 2005; (3) Smith et al. 2005; (4) Paulin-Henriksson et al. 2007; (5) Kneib et al. 1993; (6) Limousin et al. 2007; (7) Campusano et al. 2001; (8) Jee et al. 2007; (9) Gioia et al. 1998; (10) Newbury & Fahlman 1999; (11) Kausch et al. 2004; (12) Bonamente et al. 2006; (13) Maughan et al. 2008; (14) Ota & Mitsuda 2004; (15) Allen 1998; (16) Kempner & David 2004; (17) Morrison et al. 2003; (18) Dahle et al. 2002; (19) Radovich et al. 2008